Atmospheric Nitrous Oxide Variations on Centennial Time Scales During the Past Two Millennia

Yeongjun Ryu, Jinho Ahn, Ji-Woong Yang, Edward J. Brook, Axel Timmermann, Thomas Blunier, Soon-Do Hur, S. J. Kim

Global Biogeochemical Cycles

RESEARCH ARTICLE
10.1029/2020GB006568

Atmospheric Nitrous Oxide Variations on Centennial Time Scales During the Past Two Millennia

Y. Ryu[1,2], J. Ahn[1], J.-W. Yang[1,3], E. J. Brook[4], A. Timmermann[5,6], T. Blunier[7], S. Hur[8], and S.-J. Kim[8]

[1]School of Earth and Environmental Sciences, Seoul National University, Seoul, South Korea, [2]Now at Department of Geosciences, Princeton University, Princeton, NJ, USA, [3]Now at Université Paris-Saclay, CNRS, CEA, UVSQ, Laboratoire des Sciences du Climat et de l'Environnement, Institut Pierre-Simon Laplace, Gif-sur-Yvette, France, [4]College of Earth, Ocean and Atmospheric Sciences, Oregon State University, Corvallis, OR, USA, [5]Center for Climate Physics, Institute for Basic Science, Pusan, South Korea, [6]Pusan National University, Pusan, South Korea, [7]Niels Bohr Institute, University of Copenhagen, Copenhagen, Denmark, [8]Korea Polar Research Institute, Incheon, South Korea

Key Points:
- We report records of N_2O concentration for the last 2,000 yr from the Styx ice core in Antarctca and NEEM ice core in Greenland
- The data accurately reveal the timing and magnitude of N_2O variations on centennial time scales
- Variations in N_2O are associated with changes in tropical and subtropical land hydrology and marine productivity

Supporting Information:
- Supporting Information S1

Correspondence to:
J. Ahn,
jinhoahn@snu.ac.kr

Citation:
Ryu, Y., Ahn, J., Yang, J.-W., Brook, E. J., Timmermann, A., Blunier, T., et al. (2020). Atmospheric nitrous oxide variations on centennial time scales during the past two millennia. *Global Biogeochemical Cycles*, *34*, e2020GB006568. https://doi.org/10.1029/2020GB006568

Received 5 FEB 2020
Accepted 20 AUG 2020
Accepted article online 24 AUG 2020

Abstract The continuous growth of atmospheric nitrous oxide (N_2O) is of concern for its potential role in global warming and future stratospheric ozone destruction. Climate feedbacks that enhance N_2O emissions in response to global warming are not well understood, and past records of N_2O from ice cores are not sufficiently well resolved to examine the underlying climate-N_2O feedbacks on societally relevant time scales. Here, we present a new high-resolution and high-precision N_2O reconstruction obtained from the Greenland NEEM (North Greenland Eemian Ice Drilling) and the Antarctic Styx Glacier ice cores. Covering the N_2O history of the past two millennia, our reconstruction shows a centennial-scale variability of ~10 ppb. A pronounced minimum at ~600 CE coincides with the reorganizations of tropical hydroclimate and ocean productivity changes. Comparisons with proxy records suggest association of centennial- to millennial-scale variations in N_2O with changes in tropical and subtropical land hydrology and marine productivity.

Plain Language Summary Nitrous oxide (N_2O) is a greenhouse and ozone-depleting gas. The growing level of N_2O in the atmosphere is of global concern, and records of past N_2O variations can provide an important context for understanding the links between N_2O and climate change. In this study, we report new, high-quality N_2O records covering the last two millennia using ice cores obtained from Greenland and Antarctica. Our N_2O records show rapid centennial-scale changes in atmospheric N_2O and confirm a pronounced minimum near 600 CE. Comparison with climate records suggests that hydroclimate change on land and changes in marine productivity contribute to centennial- to millennial-scale N_2O variations.

1. Introduction

Improved knowledge of greenhouse gas-climate feedbacks is required to understand past and future climate changes. Nitrous oxide (N_2O) is a particularly important greenhouse gas with a global warming potential ~260 times greater than that of CO_2 for a time horizon of 100 yr (Myhre et al., 2013). With the regulation of chlorofluorocarbon emissions, N_2O is becoming the most important ozone-destroying substance in the stratosphere (Ravishankara et al., 2009). Nonetheless, the processes governing atmospheric N_2O variability still remain elusive.

Microbial production in soils and the ocean are dominant sources of atmospheric N_2O (Butterbach-Bahl et al., 2013). The atmospheric N_2O concentration is primarily regulated by the balance of these terrestrial and oceanic sources (Freing et al., 2012) with the tropical stratospheric upwelling and photolysis in the stratosphere (Khosrawi et al., 2013; Olsen et al., 2001; Prather et al., 2015). The use of nitrogen fertilizer and other industrial activities in the modern era have added extra reactive nitrogen to the global ecosystems, causing a continuous increase in atmospheric N_2O levels since the industrial revolution (Galloway et al., 2008). In addition, natural emissions are thought to be sensitive to future climate change (Battaglia & Joos, 2018; Denman et al., 2007; Martinez-Rey et al., 2015; Voigt et al., 2017).

Nitrification and denitrification are considered to be the two major pathways for natural N_2O production (Butterbach-Bahl et al., 2013; Ji et al., 2015). In the presence of molecular oxygen, ammonium (NH_4^+) can

be oxidized to nitrite (NO_2^-) and nitrate (NO_3^-) (nitrification), with N_2O as a by-product. In anoxic or suboxic conditions, denitrification reduces NO_3^- or NO_2^- into dinitrogen gas (N_2) in a stepwise fashion, with N_2O as an intermediate product. Because these microbial processes are highly dependent on temperature and oxygen levels in both marine and terrestrial environments, the feedbacks between N_2O production and climate conditions are important.

Our understanding of climate-N_2O feedbacks relies, in part, on paleoatmospheric records and modeling studies. In this context, air bubbles trapped in polar ice cores provide a unique archive for reconstructing and testing ancient atmospheric composition changes through climate history. Several detailed ice core N_2O records have been developed over the past few decades (Fischer et al., 2019; Flückiger et al., 2002, 2004; Schilt et al., 2010; Spahni et al., 2005). These records capture long-term variations, such as glacial-interglacial cycles, millennial-scale variations during the Holocene, and the N_2O responses to specific abrupt climatic events, including the preboreal transition at the end of the last glacial period and earlier Dansgaard-Oeschger events (Fischer et al., 2019; Flückiger et al., 1999, 2002; Schilt et al., 2010, 2014; Sowers et al., 2003; Spahni et al., 2005). Although previous studies reported pronounced covariability of N_2O with northern hemispheric temperature on glacial-interglacial and millennial scales (Flückiger et al., 2002; Schilt et al., 2010), available ice core N_2O records for the Holocene have not been sufficiently consistent to allow for an examination of smaller changes on submillennial time scales. Specifically, the past two millennia are thought to be affected by natural climate variability and the growing human influence. Centennial-scale variations are not well resolved in existing ice core N_2O records (MacFarling Meure et al., 2006; Prokopiou et al., 2018), apart from the strong atmospheric N_2O increase over the past 200 yr (Flückiger et al., 1999; Machida et al., 1995; Sowers et al., 2002).

To improve our understanding of the key drivers of atmospheric N_2O variability on centennial time scales, we present new high-resolution (~15 yr) ice core N_2O records from both the Greenland NEEM (North Greenland Eemian Ice Drilling) and the Antarctic Styx Glacier ice cores, which cover the past two millennia, and investigate the underlying control mechanisms.

2. Materials and Methods

2.1. Samples and Gas Chronology

Styx Glacier ice and NEEM ice were used for N_2O measurements. The climatic information of the ice coring sites is listed in supporting information Table S1. The 210.5 m long Styx Glacier ice core and firn air samples were obtained during the Korean ice core drilling campaign in 2014–2015 (Han et al., 2015). The gas age scale of the Styx Glacier record was obtained by synchronizing its CH_4 record to the West Antarctic Ice Sheet (WAIS) divide CH_4 record on the WD2014 age scale (Buizert et al., 2015). The uncertainty of the correlation is ~ ±20 yr (Yang et al., 2018). The Δage (difference in ice age and gas age) of the Styx Glacier ice was estimated to be ~318 yr (Yang et al., 2018). The gas chronology of the NEEM main ice core was also synchronized to the WD2014 age scale to solve the observed age discrepancy of ~20 yr between the NEEM-2011-S1 and WD2014 age scales (Rhodes et al., 2013) (Figure S1). The NEEM-2011-S1 core is a shallow parallel core to the NEEM main core. The estimated age difference between the main ice core and S1 ice core is less than ~5 yr (Sigl et al., 2015), smaller than the age uncertainty resulted from wiggle matching CH_4 records (~ ±20 yr). No high-resolution CH_4 data exist below 408.96 m (291 CE) (Rhodes et al., 2013). We estimated the gas age for the deeper NEEM ice by linear extrapolation of the depth-gas age relationship at depth of 338–408 m.

2.2. Ice Core N_2O Measurements

We used a high-precision measurement method (Ryu et al., 2018) to analyze both the NEEM and Styx Glacier ice and generate a composite N_2O record. Ice core samples are cut into subsamples (~20 g) in a walk-in freezer at a temperature of −20°C to prevent melting. For each depth, samples are duplicated or quadruplicated to estimate the reproducibility of measurements. Ice pieces are placed in glass flasks sealed to a Conflat Flange with a copper gasket for sealing at a high vacuum level. The flasks are then submerged into a prechilled ethanol bath (< −75°C) and evacuated to remove the ambient air in the flask and any contaminants on the ice core surface, for 50 min. After sufficient evacuation, gases in the ice core bubbles are liberated by melting. The N_2O mixing ratio of the liberated air in the headspace is measured by an

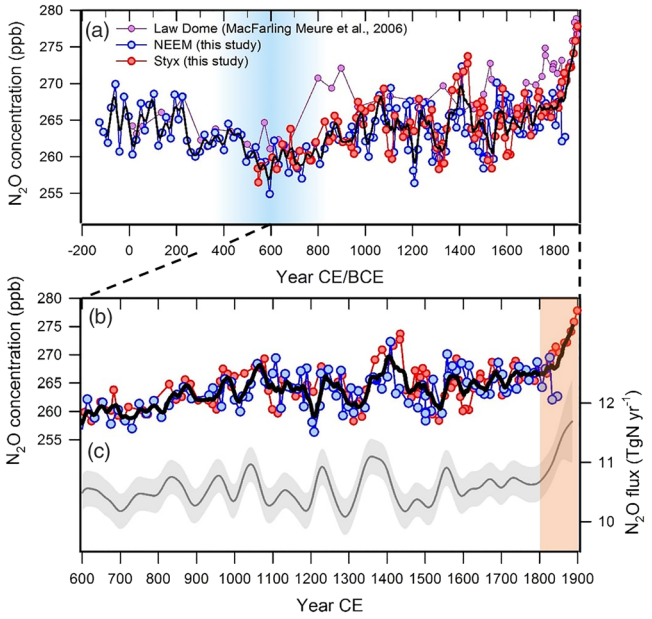

Figure 1. Atmospheric N_2O and tropical climate proxies for the past two millennia. (a) N_2O variations during the past two millennia from NEEM (blue circle), Styx Glacier (red circles) (this study), and Law Dome (MacFarling Meure et al., 2006) (purple circles) ice cores. Black solid line indicates 26 yr average of our new NEEM and Styx Glacier N_2O records. (b) N_2O concentration records between 600 and 1900 CE are plotted with (c) estimated change in N_2O flux from a two-box model (Schilt et al., 2014). Gray shading area denotes $\pm 1\sigma$ of the mean. For (b) and (c), pale orange shading after 1800 CE denotes the period considered to be strongly affected by anthropogenic emission.

Agilent 7890B Gas Chromatograph equipped with a Micro-Electron Capture Detector. Before and after the sample measurement, we analyzed a standard N_2O gas with a concentration of 329.9 ppb from the National Oceanic and Atmosphere Administration NOAA-2006A N_2O scale. Due to the high solubility of N_2O in water, we repeated the freezing-melting cycle to liberate the N_2O trapped during the extraction procedure. The additional freezing-melting step results in a ~6% correction to the total N_2O concentration.

3. Data Quality

Both ice cores have fairly high accumulation rates (NEEM: 0.22 and Styx Glacier: 0.13 m ice equivalent/yr; supporting information Table S1), resulting in a small smoothing effect on gas records due to gas diffusion and gradual bubble close-off processes in the firn layer (transition zone from snow to ice on top of the ice sheet). The estimated widths of the gas age distribution at half height from firn densification models for both ice cores are smaller than 40 yr (Buizert et al., 2012; Jang et al., 2019). Thus, both ice cores can resolve centennial-scale changes in atmospheric composition. We estimated the uncertainty of the N_2O concentration by replicating measurements with series of adjacent eight samples within ~20 cm intervals (corresponding to 1–2 yr in mean age change) and obtained pooled standard deviations of 3.4 ppb for Styx Glacier ice and 2.8 ppb for NEEM ice (supporting information Table S2). These are greater than the analytical uncertainty of 1.5 ppb which is determined from measurements of Styx replicate ice samples within 5 cm depth intervals (Ryu et al., 2018), indicating that N_2O concentration in the ice core varies in cm scales. Alteration of N_2O concentration by in situ microbial activity in the ice (Miteva et al., 2016; Rohde et al., 2008) could contribute the N_2O variations and may explain the greater scatter in longer sample interval. However, we do not believe that in situ production of N_2O can explain the centennial-scale variations we describe here, because the variations in N_2O measured in the two cores we studied are remarkably coherent (Figure 1a) on centennial time scales. The two cores have different gas age-ice age (Δage) differences (~310 yr for Styx, Jang et al., 2019, and ~188 yr for NEEM, Buizert et al., 2012), which means that dust variations would be offset differently with the gas record in each core. Instead, the agreement indicates that these centennial changes represent the true atmospheric signal. Owing to the higher anthropogenic emissions in the Northern Hemisphere, current atmospheric N_2O levels are 0.8 ppb higher in the Northern Hemisphere than in the Southern Hemisphere (Ishijima et al., 2009). However, the uncertainty of our ice core records from Greenland and Antarctica does not allow to detect such a small N_2O gradient for the preindustrial period. To focus on the joint variability in both cores, we develop a composite N_2O record by averaging the NEEM and Styx Glacier N_2O records, which were initially interpolated onto the same time axis. Our new data show subtle centennial-scale changes, which were not well resolved in previous ice core N_2O records (Fischer et al., 2019; Flückiger et al., 1999, 2002; MacFarling Meure et al., 2006; Schilt et al., 2010) (supporting information Figure S2).

4. Results

As shown in Figure 1, the composite N_2O records exhibit two distinctive features during the late preindustrial Holocene: (1) a minimum near 600 CE and (2) centennial-scale fluctuations of about 10 ppb. The 600 CE minimum was previously observed in the Law Dome ice core N_2O record, although the uncertainty of the N_2O data (± 6.5 ppb) was not sufficient to resolve the magnitude of the N_2O decrease (MacFarling Meure et al., 2006). In our measurements, N_2O from both NEEM and Styx Glacier confirms that a local minimum resides near 600 CE, thereby consolidating the finding of a substantial change in the land and/or ocean N_2O fluxes (Figure 1a). The N_2O concentration decreases from ~265 ppb at 200 CE to ~257 ppb at 600 CE.

This ~8 ppb decrease corresponds to average reduction of ~0.3 Tg N yr^{-1} in N_2O emissions. This value is calculated with a simple mass burden to mixing ratio (4.79 Tg N/ppb) (Prather et al., 2015) and the assumption that changes in the stratospheric N_2O sink are negligible (see supporting information).

Centennial-scale N_2O fluctuations are also prominent (Figure 1b). To further examine centennial-scale variations in the N_2O budget, we estimated emissions from the concentration data using a two-box model (Figure 1c). To estimate N_2O emissions, Monte Carlo simulations incorporating uncertainties in N_2O concentration and lifetime were run for each time interval (see supporting information for details). We find that emission ranges from 10.2–11.7 Tg N yr^{-1} on average, similar to the current estimates of the natural N_2O flux from both top-down and bottom-up approaches (Davidson & Kanter, 2014) (10–12 Tg N yr^{-1}). As expected, the atmospheric N_2O concentration shows a delayed response of several decades after the change in the N_2O emission (Figures 1b and 1c).

5. Discussion: N_2O and Paleoclimate

N_2O production relies on the metabolic processes of specific groups of microorganisms. Both terrestrial and marine N_2O sources are expected to respond to changes in the large-scale climate conditions. Environmental factors such as temperature and oxygen availability are believed to have significant impacts on the regulation of N_2O production. In the case of terrestrial N_2O sources, which account for ~70% of the global N_2O emissions, the water-filled pore space (WFPS) is one of the key factors controlling oxygen availability and N_2O production in the soil environments (Davidson et al., 2000). An optimum WFPS of 70–80% in the soil increases microbial activity and N_2O emissions (Bouwman et al., 2013). Tropical forest soils are the main terrestrial N_2O source (Stehfest & Bouwman, 2006; Xu et al., 2017), and the rainfall variations throughout the monsoon season have been suggested as the key factor influencing the interannual variability of the N_2O emission (Werner et al., 2007). The soil temperature is another important climate factor that can enhance terrestrial microbial N_2O production. Model studies suggest that on decadal to multidecadal time scales, temperature is the main climate parameter driving changes in terrestrial N_2O emission (Xu et al., 2012; Zaehle et al., 2011). Oceanic N_2O production is tightly associated with high primary productivity regions. Ocean systems are considered to contribute approximately 30% of natural N_2O emissions (Voss et al., 2013), and high productivity regions contribute a greater portion of the marine N_2O emissions. The eastern tropical Pacific (ETP) and Arabian Sea (AS), where considerable N_2O accumulation occurs on the upper boundary of widely developed oxygen minimum zones (OMZs) (Hamersley et al., 2007; Ito & Deutsch, 2013), are well-known major oceanic N_2O source regions. The thermocline depth and strength of the upwelling activity in these regions may influence the nutrient supply that sustains the primary productivity and, in turn, the N_2O production rate. The dissolved O_2 in upper ocean can affect N_2O production and emission variability since both denitrification and nitrification are sensitive to dissolved O_2, closely tied to aerobic remineralization of organic matter (Battaglia & Joos, 2018; Martinez-Rey et al., 2015).

The local N_2O minimum at 600 CE coincides with an overall weakening of the tropical and subtropical monsoon and lower productivity in major oceanic N_2O source regions, as indicated by a variety of palaeoclimate proxy records (Figure 2 and supporting information Figure S3). The N_2O level continuously decreased until 600 CE and then increased until 1200 CE. The timing of this N_2O minimum is coincident with reduced precipitation in the tropical land N_2O source areas, including subtropical China (Wang et al., 2005), Southeast Asia (Steinke et al., 2014; Wurtzel et al., 2018), India (Anderson et al., 2002, 2010; Gupta et al., 2003), and central America (Bhattacharya et al., 2015; Curtis et al., 1996). Because the optimum conditions for microbial N_2O production requires a high level of soil moisture (~70% to 80%) to achieve low O_2 availability, a weakening in the monsoon strength in the tropical land source areas may decrease N_2O production. The hydroclimate proxies in South America are not sufficiently consistent to confirm changes in the rainfall patterns at 600 CE; however, some of them suggest an abnormally drier climate (Bird et al., 2011; Kanner et al., 2013; Novello et al., 2012), illustrating a potential regional contribution of hydroclimate changes in South America to lower N_2O emissions in this period. There are a few available hydroclimate proxy records in central Europe (Fohlmeister et al., 2012) and central Africa (Shanahan et al., 2009; Wolff et al., 2011), resolving the last 2,000 yr; however, the climate in these areas became wetter or showed no significant changes in this period, possibly contributing to the increase in the regional N_2O emission. The marine

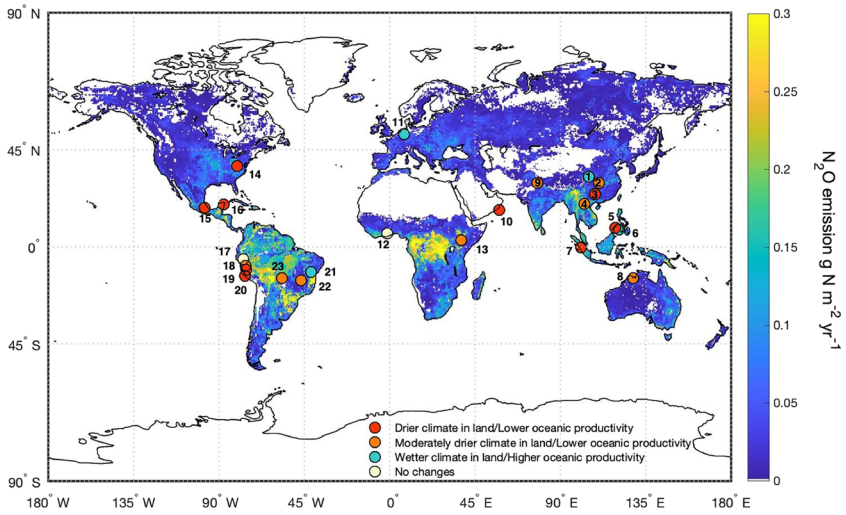

Figure 2. Deviation in land hydroclimate and oceanic productivity between 400 and 800 CE from preindustrial average. Red circles (cyan circles) represent much drier conditions in land or lower oceanic productivity (wetter condition in land or higher oceanic productivity) between 400 and 800 CE (average z score > 0.5 or $z < -0.5$). Orange circles indicate the regions where the climate changed to a moderately drier condition or lower productivity during this period ($0.5 > z > 0.3$). Pale yellow marks the regions with no significant changes ($0.3 > z$). All proxy records marked in this map were normalized, and the resulting z scores were used for analysis. The background map shows the modeled terrestrial N_2O emission in preindustrial times (Xu et al., 2017). Proxies: 1. Wanxiang cave (Zhang et al., 2008), 2. Heshang cave (Hu et al., 2008), 3. Dongge cave (Wang et al., 2005), 4. Tham Doun Mai cave (Wang et al., 2019), 5. Sumba Island (Steinke et al., 2014), 6. Liang Luar cave (Griffiths et al., 2009, 2016), 7. Tannga cave (Wurtzel et al., 2018), 8. KNI-51 cave (Denniston et al., 2016), 9. Sahiya cave (Kathayat et al., 2017), 10. Arabian Sea (RC 2735, RC 2730 cores) (Anderson et al., 2002, 2010; Gupta et al., 2003), 11. Bunker cave (Fohlmeister et al., 2012), 12. Lake Bosumtwi (Shanahan et al., 2009), 13. Lake Challa (Wolff et al., 2011), 14. Buckeye Creek cave (Hardt et al., 2010), 15. Laguna de Aljojuca (Bhattacharya et al., 2015), 16. Lake Punta Laguna (Curtis et al., 1996), 17. Tigre Perdido cave (van Breukelen et al., 2008), 18. Laguna Pumacocha (Bird et al., 2011), 19. Huagapo cave (Kanner et al., 2013), 20. Peru off (B0506-14 core) (Salvatteci et al., 2014), 21. Diva de Maura cave (Novello et al., 2012), 22. Tamboril cave (Wortham et al., 2017), and 23. Pau d'Alho cave (Novello et al., 2016). All proxies records were normalized to their mean value covering the period between 500 BCE and 1800 CE. Wanxiang, Tham Doun Mai, and Pau d'Alho cave records, which do not cover the entire period, were normalized to the average over their maximum ages (CE 192, BCE 51, CE 492).

sediment records from AS and the equatorial eastern Pacific, which account for a significant portion of the oceanic N_2O emissions, show an overall reduction in productivity near 600 CE, which would further lead to a reduction in the N_2O emission (Figure 2).

To deduce the extent and patterns of the hydrological changes on land, we compared our N_2O composite with selected temporally well-resolved hydroclimate proxies (Figure 3). Among the cave speleothem proxy records ($\delta^{18}O$ of speleothem calcium carbonate) in China, representing the strength of the Eastern Asian Summer Monsoon (EASM), the lower-latitudinal cave speleothem records from Dongge cave (Wang et al., 2005) (25.28°N) show a minimum near ~500 CE, while Heshang (Hu et al., 2008) (30.27°N) and Wanxiang (Zhang et al., 2008) caves (33.32°N) records do not share this pattern (supporting information Figure S4). The Wanxiang cave records (Zhang et al., 2008) indicate an even stronger EASM between 400 and 800 CE. This latitudinal discrepancy in the EASM proxies is suggested to result from changes in the width of the tropical rainfall belt with the migration of the Intertropical Convergence Zones (Denniston et al., 2016). Thus, the weakening of the EASM strength was possibly constrained to the tropical and subtropical regions.

The western tropical Pacific and Indian subcontinent also experienced diminishing monsoon activity; the Indonesian-Australian Summer Monsoon (IASM) and Indian Summer Monsoon (ISM) weakened between 400 and 800 CE (Figures 3b and 3c and supporting information Figure S3). The lake sediment titanium to calcium ratio (Ti/Ca) records from Sumba Island (9.22°S, 118.89°E), the southeastern part of Indonesia, documented the past changes in the summer monsoon rainfall and showed a strongly reduced IASM rainfall near 600 CE (Steinke et al., 2014) (Figure 3b). Highly resolved tropical Australian cave records (Denniston

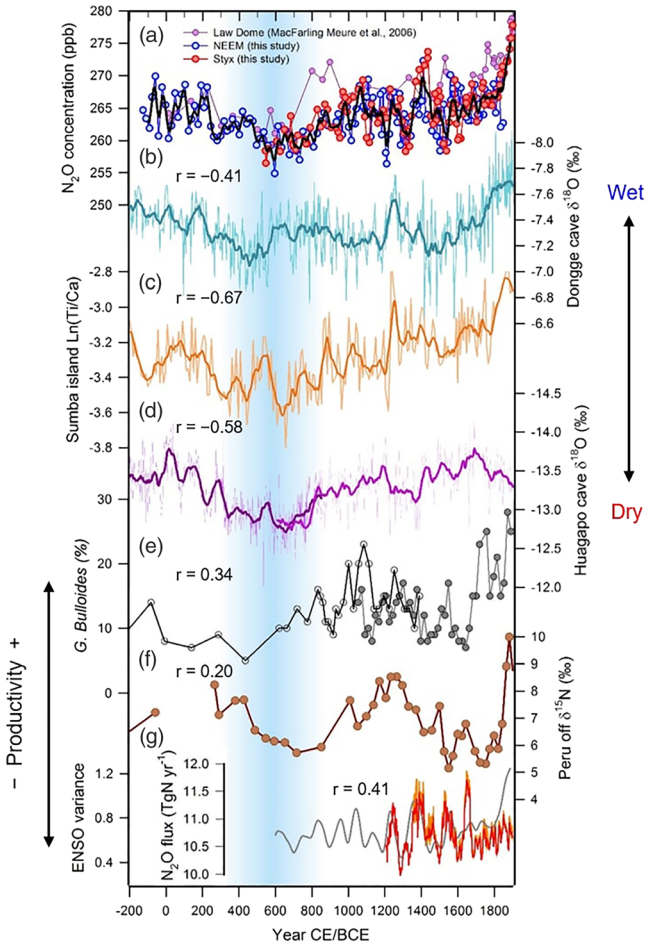

Figure 3. Comparison of N_2O with land hydroclimate, oceanic productivity, and El Niño–Southern Oscillation (ENSO) proxies. (a) N_2O concentration reconstructed in this study (marks are same with Figure 1). (b) Cave speleothem $\delta^{18}O$ records from Dongge cave, south China (Wang et al., 2005) (c) Ti/Ca content of sediment core from Sumba island, Indonesia (Steinke et al., 2014). (d) Cave speleothem $\delta^{18}O$ records from Huagapo cave (P00-H1, P09-H2 cores), Peruvian Andes (Kanner et al., 2013). (e) *G. bulloides* content in Arabian Sea sediment cores (Anderson et al., 2010; Gupta et al., 2003) (filled circles: RC2730, RC2735 cores, Anderson et al., 2010; open circles: 723A core, Gupta et al., 2003). (f) $\delta^{15}N$ of organic matter in off Peru sediment core (Salvatteci et al., 2014). (g) Combined tree ring-based 31 yr running variance of interannual-scale variability ENSO records (red line) with their $\pm1\sigma$ uncertainty (pale red shading) (Liu et al., 2017). N_2O flux is plotted on same panel (gray line). (b–d) For clarity, highly resolved records are smoothed with a moving average technique with a time window of 50 yr to highlight multidecadal variations (thick solid lines). Pale blue shading represents the period of the lowest N_2O level during the last two millennia. Correlation coefficients between each proxy and N_2O concentration (b–f) or N_2O flux and ENSO variance (g) are denoted.

et al., 2016) and Sumatra Island (Wurtzel et al., 2018) supported the weakened IASM in this period. Principal component analysis on the Flores cave speleothem multiproxies from southeast Indonesia shows a drier hydrology during this period (Griffiths et al., 2016); however, it explains only ~50% of the variation pattern, and the oxygen isotope records (Griffiths et al., 2009) ($\delta^{18}O$ of calcium carbonates) from the Flores speleothem agree with a weakened IASM between 400 and 800 CE.

Like the tropical and subtropical western Pacific regions, whose hydrology is largely affected by the monsoon, the precipitation in the Amazon River basin is also greatly controlled by South American Summer Monsoon (SASM). Speleothem records from Huagapo cave (11.27°S, 75.79°W) in the Eastern Andes show a weakening of the SASM during the N_2O minimum at 600 CE (Kanner et al., 2013) (Figure 3d); however, other SASM proxies are not sufficiently consistent to confirm its weakened strength at 600 CE (Figure 2 and supporting information Figure S3). Although our interpretation of these hydroclimate proxies is limited by the discrepancies among the proxy records, a large portion of the tropical and subtropical monsoon regions appear to indicate a change toward drier conditions near 600 CE.

What caused these globally diminishing monsoon activities at 600 CE is unclear; however, hydroclimate change and the associated reduced soil moisture content in the tropical N_2O source regions likely contributed to the reductions in the terrestrial N_2O emissions. During this period, the northern hemispheric temperature is believed to be lower than average (Ljungqvist, 2010; Mann & Jones, 2003; Moberg et al., 2005) (supporting information Figure S5), which could further subdue the terrestrial N_2O emission by suppressing microbial activity. Previous work suggested that northern hemispheric temperature change caused millennial-scale N_2O changes in the Holocene, showing parallel variation with N_2O (Flückiger et al., 2002; Schilt et al., 2010). However, a quantitative estimation of the temperature change is difficult owing to the spatially dispersed temperature proxy records.

The weakening of the ISM prevents upwelling and reduces the primary productivity in the AS, likely leading to decreased N_2O production owing to the reduction in organic matter input, which is required for denitrification. The abundance of the planktonic foraminifera *Globigerina bulloides* in a sediment core from AS (Anderson et al., 2002, 2010; Gupta et al., 2003) (Figure 3e) shows a minimum at 600 CE, reflecting the reduction in the primary productivity, consistent with the reduction in the marine N_2O flux from AS. Similarly, the nitrogen isotope ratios ($\delta^{15}N$) of organic matter in a sediment core off Peru suggest a reduction in the primary productivity and weakened OMZ development in ETP near 600 CE, followed by a gradual strengthening (Salvatteci et al., 2014) (Figure 3f). OMZs are the regions where active nitrogen loss (both denitrification and anammox) take place, contributing ~4% of the estimated oceanic N_2O production (Battaglia & Joos, 2018). In addition, the combination of aerobic remineralization of organic matter followed by nitrification results in strong regional N_2O production where OMZs are well developed (Yang et al., 2020). Thus, a reduction in the OMZ in ETP and AS could also lead to a decrease in oceanic N_2O emissions. In summary, both terrestrial and marine palaeoclimate records suggest that the reorganization of

tropical rainfall and wind patterns may have contributed to the marked decrease in N_2O fluxes into the atmosphere near 600 CE.

This period was thought to be affected by changes in the periodical North Atlantic cooling events, known as Bond events (Bond et al., 2001). The North Atlantic cooling can be linked to the changes in Asian southeast monsoon and AS productivity (Gupta et al., 2003). Thus, the North Atlantic cooling can be associated with the subdued productivity of N_2O near 600 CE. Dongge cave records may indicate a possible linkage between Asian monsoon strength and the North Atlantic cooling (Wang et al., 2005). Possible changes in climate during this time period include Pacific sea surface temperature (SST) gradient changes (Kanner et al., 2013) and northern hemispheric temperature changes (Kathayat et al., 2017), both of which could contribute to the reorganization of the tropical and subtropical hydroclimates.

On centennial time scales, regional monsoon proxies and oceanic productivity records are not highly correlated with our N_2O flux estimates. The low correlation among the N_2O flux and climate proxies might be because of age uncertainty of proxies and our N_2O data, which can reach several decades in age difference between the N_2O and the palaeoproxy data. Tropical rainfall change in such a short-term temporal scale may be spatially inconsistent and possibly lead to the lack of predominance in the N_2O emission. The only meaningful correlation for the N_2O flux was achieved with the annually resolved central Pacific El Niño–Southern Oscillation (ENSO) proxies (Figure 3g). ENSO variance records based on Taiwan tree ring $\delta^{18}O$ show in-phase correlation with the calculated N_2O flux (Liu et al., 2017) ($r = 0.41$). The centennial-scale decrease in the N_2O flux corresponds to a suppressed ENSO variance, whereas the periods of high ENSO variance coincide with enhanced N_2O emission. A correlation coefficient r of 0.41 is a conservative value, given the relative age uncertainty between the records. While we cannot address the physical mechanism between the central Pacific ENSO and N_2O flux changes, it may reflect the relationship between the N_2O production and climate variability in low-latitudinal regions.

The discussion above focuses on N_2O production changes rather than changes in sinks related to photochemical decomposition in the stratosphere. The fluctuations in our N_2O records appear to match with proxies of solar activity changes. N_2O concentrations are in phase with total solar irradiance reconstruction data (Steinhilber et al., 2009), showing low levels of N_2O during the solar minima events of the past millennium (supporting information Figure S6). A recent study reported that the N_2O lifetime varies with solar activity (Prather et al., 2015); the lifetime of N_2O decreases in solar maxima (while it increases in solar minima), indicating more rapid N_2O loss and decrease of N_2O during the solar maxima. However, our observation is a positive correlation between N_2O and solar activity. This may imply that the changes in N_2O loss due to solar activity are not large enough to counterbalance changes in N_2O sources during the past two millennia.

To better understand the physical linkage between climate and N_2O changes, further numerical modeling experiments are required as well as chemical and isotopic data. The isotopic composition of N_2O molecule ($\delta^{15}N$, $\delta^{18}O$, and site preference) has been used as the footprint for distinguishing its sources and production processes (Fischer et al., 2019; Prokopiou et al., 2018; Schilt et al., 2014; Sutka et al., 2006), and it may provide a way to deduce the mechanistic explanation for the N_2O variations. However, published N_2O isotope data do not have sufficient temporal resolution and precision to facilitate the investigation of the relative contribution of marine and terrestrial sources or microbial production mechanisms (nitrification vs. denitrification) on submillenial time scales (Prokopiou et al., 2018). Future studies of N_2O isotopologues and higher-resolution N_2O isotope records will be very useful to improve our understanding of the connection between N_2O emissions and regional and large-scale climate.

6. Conclusion

We present the submillennial-scale N_2O variations during the past two millennia with highly resolved ice core records and evaluate their possible causes. Our data show variability of ~10 ppb on a centennial time scale. A pronounced local minimum at ~600 CE coincides with the changes in tropical hydroclimate and ocean productivity. Both terrestrial and marine N_2O production rate changes in response to climate are likely explanations for the atmospheric N_2O concentration changes. Disentangling the underlying changes in terrestrial and marine N_2O production rate changes requires further analysis of N_2O isotopes and targeted modeling experiments with state-of-the-art Earth system models.

Data Availability Statement

The data are available at NOAA (National Oceanic and Atmospheric Administration) Paleoclimatology website (https://www.ncdc.noaa.gov/paleo-search/study/30752).

Acknowledgments
We thank Soonil An and Seok-Woo Son for valuable comments. Financial support was provided by the Basic Science Research Program through the National Research Foundation of Korea (NRF) (NRF-2018R1A2B3003256). A. T. was supported by the Institute for Basic Science (Project Code IBS-R028-D1).

References

Anderson, D. M., Baulcomb, C. K., Duvivier, A. K., & Gupta, A. K. (2010). Indian summer monsoon during the last two millennia. *Journal of Quaternary Science*, *25*(6), 911–917. https://doi.org/10.1002/jqs.1369

Anderson, D. M., Overpeck, J. T., & Gupta, A. K. (2002). Increase in the Asian southwest monsoon during the past four centuries. *Science*, *297*(5581), 596–599. https://doi.org/10.1126/science.1072881

Battaglia, G., & Joos, F. (2018). Marine N_2O emissions from nitrification and denitrification constrained by modern observations and projected in multimillennial global warming simulations. *Global Biogeochemical Cycles*, *32*, 92–121. http://doi.org/10.1002/2017GB005671

Bhattacharya, T., Byrne, R., Böhnel, H., Wogau, K., Kienel, U., Ingram, B. L., & Zimmerman, S. (2015). Cultural implications of late Holocene climate change in the Cuenca Oriental, Mexico. *Proceedings of the National Academy of Sciences of the United States of America*, *112*(6), 1693–1698. https://doi.org/10.1073/pnas.1405653112

Bird, B. W., Abbott, M. B., Vuille, M., Rodbell, D. T., Stansell, N. D., & Rosenmeier, M. F. (2011). A 2,300-year-long annually resolved record of the South American summer monsoon from the Peruvian Andes. *Proceedings of the National Academy of Sciences of the United States of America*, *108*(21), 8583–8588. https://doi.org/10.1073/pnas.1003719108

Bond, G., Kromer, B., Beer, J., Muscheler, R., Evans, M. N., Showers, W., et al. (2001). Persistent solar influence on North Atlantic climate during the Holocene. *Science*, *294*(5549), 2130–2136. https://doi.org/10.1126/science.1065680

Bouwman, A. F., Beusen, A. H. W., Griffioen, J., Van Groenigen, J. W., Hefting, M. M., Oenema, O., et al. (2013). Global trends and uncertainties in terrestrial denitrification and N_2O emissions. *Philosophical Transactions of the Royal Society, B: Biological Sciences*, *368*, 20130112. https://doi.org/10.1098/rstb.2013.0112

Buizert, C., Cuffey, K. M., Severinghaus, J. P., Baggenstos, D., Fudge, T. J., Steig, E. J., et al. (2015). The WAIS divide deep ice core WD2014 chronology—Part 1: Methane synchronization (68-31 ka BP) and the gas age-ice age difference. *Climate of the Past*, *11*(2), 153–173. https://doi.org/10.5194/cp-11-153-2015

Buizert, C., Martinerie, P., Petrenko, V. V., Severinghaus, J. P., Trudinger, C. M., Witrant, E., et al. (2012). Gas transport in firn: Multiple-tracer characterisation and model intercomparison for NEEM, northern Greenland. *Atmospheric Chemistry and Physics*, *12*(9), 4259–4277. https://doi.org/10.5194/acp-12-4259-2012

Butterbach-Bahl, K., Baggs, E. M., Dannenmann, M., Kiese, R., & Zechmeister-Boltenstern, S. (2013). Nitrous oxide emissions from soils: How well do we understand the processes and their controls? *Philosophical Transactions of the Royal Society, B: Biological Sciences*, *368*(1621), 20130122. https://doi.org/10.1098/rstb.2013.0122

Curtis, J. H., Hodell, D. A., & Brenner, M. (1996). Climate variability on the Yucatan Peninsula (Mexico) during the past 3500 years, and implications for Maya cultural evolution. *Quaternary Research*, *46*(1), 37–47. https://doi.org/10.1006/qres.1996.0042

Davidson, E. A., & Kanter, D. (2014). Inventories and scenarios of nitrous oxide emissions. *Environmental Research Letters*, *9*(10), 105012. https://doi.org/10.1088/1748-9326/9/10/105012

Davidson, E. A., Keller, M., Erickson, H. E., Verchot, L. V., & Veldkamp, E. (2000). Testing a conceptual model of soil emissions of nitrous and nitric oxides. *Bioscience*, *50*(8), 667. https://doi.org/10.1641/0006-3568(2000)050[0667:tacmos]2.0.co;2

Denman, K. L., Brasseur, G., Chidthaisong, A., Ciais, P., Cox, P. M., Dickinson, R. E., et al. (2007). Couplings between changes in the climate system and biogeochemistry coordinating lead authors: This chapter should be cited as. In *Climate change 2007: The physical science basis. Contribution of Working Group I to the Fourth Assessment Report of the Intergovernmental Panel on Climate Change* (pp. 500–587). Cambridge, United Kingdom and New York, NY, USA: Cambridge University Press. Retrieved from. https://www.globalcarbonproject.org/global/pdf/AR4WG1_Pub_Ch07.pdf

Denniston, R. F., Ummenhofer, C. C., Wanamaker, A. D., Lachniet, M. S., Villarini, G., Asmerom, Y., et al. (2016). Expansion and contraction of the Indo-Pacific tropical rain belt over the last three millennia. *Scientific Reports*, *6*(1), 34485. https://doi.org/10.1038/srep34485

Fischer, H., Schmitt, J., Bock, M., Seth, B., Joos, F., Spahni, R., et al. (2019). N_2O changes from the Last Glacial Maximum to the preindustrial—Part 1: Quantitative reconstruction of terrestrial and marine emissions using N_2O stable isotopes in ice cores. *Biogeosciences*, *16*(20), 3997–4021. https://doi.org/10.5194/bg-16-3997-2019

Flückiger, J., Blunier, T., Stauffer, B., Chappellaz, J., Spahni, R., Kawamura, K., et al. (2004). N_2O and CH_4 variations during the last glacial epoch: Insight into global processes. *Global Biogeochemical Cycles*, *18*, GB1020. https://doi.org/10.1029/2003GB002122

Flückiger, J., Dällenbach, A., Blunier, T., Stauffer, B., Stocker, T. F., Raynaud, D., & Barnola, J. M. (1999). Variations in atmospheric N_2O concentration during abrupt climatic changes. *Science*, *285*(5425), 227–230. https://doi.org/10.1126/science.285.5425.227

Flückiger, J., Monnin, E., Stauffer, B., Schwander, J., Stocker, T. F., Chappellaz, J., et al. (2002). High-resolution Holocene N_2O ice core record and its relationship with CH_4 and CO_2. *Global Biogeochemical Cycles*, *16*(1), 1010. https://doi.org/10.1029/2001GB001417

Fohlmeister, J., Schröder-Ritzrau, A., Scholz, D., Spötl, C., Riechelmann, D. F. C., Mudelsee, M., et al. (2012). Bunker Cave stalagmites: An archive for central European Holocene climate variability. *Climate of the Past*, *8*(5), 1751–1764. https://doi.org/10.5194/cp-8-1751-2012

Freing, A., Wallace, D. W. R., & Bange, H. W. (2012). Global oceanic production of nitrous oxide. *Philosophical Transactions of the Royal Society, B: Biological Sciences*, *367*(1593), 1245–1255. https://doi.org/10.1098/rstb.2011.0360

Galloway, J. N., Townsend, A. R., Erisman, J., Bekunda, M., Cai, Z., Freney, J. R., et al. (2008). Transformation of the nitrogen cycle: Recent trends, questions, and potential solutions. *Science*, *320*(5878), 889–892. http://doi.org/10.1126/science.1136674

Griffiths, M. L., Drysdale, R. N., Gagan, M. K., Zhao, J. X., Ayliffe, L. K., Hellstrom, J. C., et al. (2009). Increasing Australian-Indonesian monsoon rainfall linked to early Holocene sea-level rise. *Nature Geoscience*, *2*(9), 636–639. https://doi.org/10.1038/ngeo605

Griffiths, M. L., Kimbrough, A. K., Gagan, M. K., Drysdale, R. N., Cole, J. E., Johnson, K. R., et al. (2016). Western Pacific hydroclimate linked to global climate variability over the past two millennia. *Nature Communications*, *7*, 11719. https://doi.org/10.1038/ncomms11719

Gupta, A. K., Anderson, D. M., & Overpeck, J. T. (2003). Abrupt changes in the Asian southwest monsoon during the Holocene and their links to the North Atlantic Ocean. *Nature*, *421*(6921), 354–357. https://doi.org/10.1038/nature01340

Hamersley, M. R., Lavik, G., Woebken, D., Rattray, J. E., Lam, P., Hopmans, E. C., et al. (2007). Anaerobic ammonium oxidation in the Peruvian oxygen minimum zone. *Limnology and Oceanography*, *52*(3), 923–933. https://doi.org/10.4319/lo.2007.52.3.0923

Han, Y., Jun, S. J., Miyahara, M., Lee, H., Ahn, J., Chung, J. W., et al. (2015). Shallow ice-core drilling on Styx glacier, northern Victoria Land, Antarctica in the 2014–2015 summer. *Journal of the Geological Society of Korea*, *51*, 343. https://doi.org/10.14770/jgsk.2015.51.3.343

Hardt, B., Rowe, H. D., Springer, G. S., Cheng, H., & Edwards, R. L. (2010). The seasonality of east central North American precipitation based on three coeval Holocene speleothems from southern West Virginia. *Earth and Planetary Science Letters*, *295*(3–4), 342–348. https://doi.org/10.1016/j.epsl.2010.04.002

Hu, C., Henderson, G. M., Huang, J., Xie, S., Sun, Y., & Johnson, K. R. (2008). Quantification of Holocene Asian monsoon rainfall from spatially separated cave records. *Earth and Planetary Science Letters*, *266*(3–4), 221–232. https://doi.org/10.1016/j.epsl.2007.10.015

Ishijima, K., Nakazawa, T., & Aoki, S. (2009). Variations of atmospheric nitrous oxide concentration in the northern and western Pacific. *Tellus Series B: Chemical and Physical Meteorology*, *61*(2), 408–415. https://doi.org/10.1111/j.1600-0889.2008.00406.x

Ito, T., & Deutsch, C. (2013). Variability of the oxygen minimum zone in the tropical North Pacific during the late twentieth century. *Global Biogeochemical Cycles*, *27*, 1119–1128. https://doi.org/10.1002/2013GB004567

Jang, Y., Hong, S., Buizert, C., Lee, H. G., Han, S. Y., Yang, J. W., et al. (2019). Very old firn air linked to strong density layering at Styx Glacier, coastal Victoria land, East Antarctica. *The Cryosphere*, *13*(9), 2407–2419. https://doi.org/10.5194/tc-13-2407-2019

Ji, Q., Babbin, A. R., Jayakumar, A., Oleynik, S., & Ward, B. B. (2015). Nitrous oxide production by nitrification and denitrification in the eastern tropical South Pacific oxygen minimum zone. *Geophysical Research Letters*, *42*, 10,755–10,764. https://doi.org/10.1002/2015GL066853

Kanner, L. C., Burns, S. J., Cheng, H., Edwards, R. L., & Vuille, M. (2013). High-resolution variability of the South American summer monsoon over the last seven millennia: Insights from a speleothem record from the central Peruvian Andes. *Quaternary Science Reviews*, *75*, 1–10. https://doi.org/10.1016/j.quascirev.2013.05.008

Kathayat, G., Cheng, H., Sinha, A., Yi, L., Li, X., Zhang, H., et al. (2017). The Indian monsoon variability and civilization changes in the Indian subcontinent. *Science Advances*, *3*, e1701296. https://doi.org/10.1126/sciadv.1701296

Khosrawi, F., Muller, R., Urban, J., Proffitt, M. H., Stiller, G., Kiefer, M., et al. (2013). Assessment of the interannual variability and influence of the QBO and upwelling on tracer-tracer distributions of N_2O and O_3 in the tropical lower stratosphere. *Atmospheric Chemistry and Physics*, *13*(7), 3619–3641. http://doi.org/10.5194/acp-13-3619-2013

Liu, Y., Cobb, K. M., Song, H., Li, Q., Li, C. Y., Nakatsuka, T., et al. (2017). Recent enhancement of central Pacific El Niño variability relative to last eight centuries. *Nature Communications*, *8*, 15386. https://doi.org/10.1038/ncomms15386

Ljungqvist, F. C. (2010). A new reconstruction of temperature variability in the extra-tropical Northern Hemisphere during the last two millennia. *Geografiska Annaler. Series A, Physical Geography*, *92*(3), 339–351. https://doi.org/10.1111/j.1468-0459.2010.00399.x

MacFarling Meure, C., Etheridge, D., Trudinger, C., Steele, P., Langenfelds, R., Van Ommen, T., et al. (2006). Law Dome CO_2, CH_4 and N_2O ice core records extended to 2000 years BP. *Geophysical Research Letters*, *33*, L14810. https://doi.org/10.1029/2006GL026152

Machida, T., Nakazawa, T., Fujii, Y., Aoki, S., & Watanabe, O. (1995). Increase in the atmospheric nitrous oxide concentration during the last 250 years. *Geophysical Research Letters*, *22*(21), 2921–2924. https://doi.org/10.1029/95GL02822

Mann, M. E., & Jones, P. D. (2003). Global surface temperatures over the past two millennia. *Geophysical Research Letters*, *30*(15), 1820. https://doi.org/10.1029/2003GL017814

Martinez-Rey, J., Bopp, L., Gehlen, M., Tagliabue, A., & Gruber, N. (2015). Projections of oceanic N_2O emissions in the 21st century using the IPSL Earth system model. *Biogeosciences*, *12*(13), 4133–4148. http://doi.org/10.5194/bg-12-4133-2015

Miteva, V., Sowers, T., Schüpbach, S., Fischer, H., & Brenchley, J. (2016). Geochemical and microbiological studies of nitrous oxide variations within the new NEEM Greenland ice core during the last glacial period. *Geomicrobiology Journal*, *33*(8), 647–660. http://doi.org/10.1080/014905451.2015.1074321

Moberg, A., Sonechkin, D. M., Holmgren, K., Datsenko, M. H., & Karlén, W. (2005). Highly variable Northern Hemisphere temperatures reconstructed from low- and high-resolution proxy data. *Nature*, *433*(7026), 613–617. https://doi.org/10.1038/nature03265

Myhre, G. D., Shindell, F.-M., Bréon, W., Collins, J., Fuglestvedt, J., Huang, J., et al. (2013). Anthropogenic and natural radiative forcing. In T. F. Stocker, et al., (Eds.), *Climate change 2013: The physical science basis. Contribution of Working Group I to the Fifth Assessment Report of the Intergovernmental Panel on Climate Change* (pp. 659–740). Cambridge, United Kingdom and New York, NY, USA: University Press.

Novello, V. F., Cruz, F. W., Karmann, I., Burns, S. J., Stríkis, N. M., Vuille, M., et al. (2012). Multidecadal climate variability in Brazil's Nordeste during the last 3000 years based on speleothem isotope records. *Geophysical Research Letters*, *39*, L23706. https://doi.org/10.1029/2012GL053936

Novello, V. F., Vuille, M., Cruz, F. W., Stríkis, N. M., De Paula, M. S., Edwards, R. L., et al. (2016). Centennial-scale solar forcing of the South American monsoon system recorded in stalagmites. *Scientific Reports*, *6*, 24762. https://doi.org/10.1038/srep24762

Olsen, S. C., McLinden, C. A., & Prather, M. J. (2001). Stratospheric N_2O-NO_y system: Testing uncertainties in a three-dimensional framework. *Journal of Geophysical Research*, *106*(D22), 28,771–28,784. https://doi.org/10.1029/2001JD000559

Prather, M. J., Hsu, J., Deluca, N. M., Jackman, C. H., Oman, L. D., Douglass, A. R., et al. (2015). Measuring and modeling the lifetime of nitrous oxide including its variability. *Journal of Geophysical Research: Atmospheres*, *120*, 5693–5705. https://doi.org/10.1002/2015JD023267

Prokopiou, M., Sapart, C. J., Rosen, J., Sperlich, P., Blunier, T., Brook, E., et al. (2018). Changes in the isotopic signature of atmospheric nitrous oxide and its global average source during the last three millennia. *Journal of Geophysical Research: Atmospheres*, *123*, 10,757–10,773. https://doi.org/10.1029/2018JD029008

Ravishankara, A. R., Daniel, J. S., & Portmann, R. W. (2009). Nitrous oxide (N_2O): The dominant ozone-depleting substance emitted in the 21st century. *Science*, *326*(5949), 123–125. https://doi.org/10.1126/science.1176985

Rhodes, R. H., Faïn, X., Stowasser, C., Blunier, T., Chappellaz, J., McConnell, J. R., et al. (2013). Continuous methane measurements from a late Holocene Greenland ice core: Atmospheric and in-situ signals. *Earth and Planetary Science Letters*, *368*, 9–19. https://doi.org/10.1016/j.epsl.2013.02.034

Rohde, R. A., Price, P. B., Bay, R. C., & Bramall, N. E. (2008). In situ microbial metabolism as a cause of gas anomalies in ice. *Proceedings of the National Academy of Sciences of the United States of America*, *105*(25), 8667–8672. https://doi.org/10.1073/pnas.0803763105

Ryu, Y., Ahn, J., & Yang, J. W. (2018). High-precision measurement of N_2O concentration in ice cores. *Environmental Science and Technology*, *52*(2), 731–738. https://doi.org/10.1021/acs.est.7b05250

Salvatteci, R., Gutiérrez, D., Field, D., Sifeddine, A., Ortlieb, L., Bouloubassi, I., et al. (2014). The response of the Peruvian upwelling ecosystem to centennial-scale global change during the last two millennia. *Climate of the Past*, *10*(2), 715–731. https://doi.org/10.5194/cp-10-715-2014

Schilt, A., Baumgartner, M., Schwander, J., Buiron, D., Capron, E., Chappellaz, J., et al. (2010). Atmospheric nitrous oxide during the last 140,000 years. *Earth and Planetary Science Letters*, *300*(1–2), 33–43. https://doi.org/10.1016/j.epsl.2010.09.027

Schilt, A., Brook, E. J., Bauska, T. K., Baggenstos, D., Fischer, H., Joos, F., et al. (2014). Isotopic constraints on marine and terrestrial N_2O emissions during the last deglaciation. *Nature*, *516*(7530), 234–237. https://doi.org/10.1038/nature13971

Shanahan, T. M., Overpeck, J. T., Anchukaitis, K. J., Beck, J. W., Cole, J. E., Dettman, D. L., et al. (2009). Atlantic forcing of persistent drought in West Africa. *Science*, *324*(5925), 377–380. https://doi.org/10.1126/science.1166352

Sigl, M., Winstrup, M., McConnell, J. R., Welten, K. C., Plunkett, G., Ludlow, F., et al. (2015). Timing and climate forcing of volcanic eruptions for the past 2,500 years. *Nature*, *523*(7562), 543–549. https://doi.org/10.1038/nature14565

Sowers, T., Alley, R. B., & Jubenville, J. (2003). Ice core records of atmospheric N_2O covering the last 106,000 years. *Science*, *301*(5635), 945–948. https://doi.org/10.1126/science.1085293

Sowers, T., Rodebaugh, A., Yoshida, N., & Toyoda, S. (2002). Extending records of the isotopic composition of atmospheric N_2O back to 1800 A.D. from air trapped in snow at the South Pole and the Greenland Ice Sheet Project II ice core. *Global Biogeochemical Cycles*, *16*(4), 1129. https://doi.org/10.1029/2002GB001911

Spahni, R., Chappellaz, J., Stocker, T. F., Loulergue, L., Hausammann, G., Kawamura, K., et al. (2005). Atmospheric science: Atmospheric methane and nitrous oxide of the late Pleistocene from Antarctic ice cores. *Science*, *310*(5752), 1317–1321. https://doi.org/10.1126/science.1120132

Stehfest, E., & Bouwman, L. (2006). N_2O and NO emission from agricultural fields and soils under natural vegetation: Summarizing available measurement data and modeling of global annual emissions. *Nutrient Cycling in Agroecosystems*, *74*(3), 207–228. https://doi.org/10.1007/s10705-006-9000-7

Steinhilber, F., Beer, J., & Fröhlich, C. (2009). Total solar irradiance during the Holocene. *Geophysical Research Letters*, *36*, L19704. https://doi.org/10.1029/2009GL040142

Steinke, S., Mohtadi, M., Prange, M., Varma, V., Pittauerova, D., & Fischer, H. W. (2014). Mid- to Late-Holocene Australian-Indonesian summer monsoon variability. *Quaternary Science Reviews*, *93*, 142–154. https://doi.org/10.1016/j.quascirev.2014.04.006

Sutka, R. L., Ostrom, N. E., Ostrom, P. H., Breznak, J. A., Gandhi, H., Pitt, A. J., & Li, F. (2006). Distinguishing nitrous oxide production from nitrification and denitrification on the basis of isotopomer abundances. *Applied and Environmental Microbiology*, *72*(1), 638–644. https://doi.org/10.1128/AEM.72.1.638-644.2006

van Breukelen, M. R., Vonhof, H. B., Hellstrom, J. C., Wester, W. C. G., & Kroon, D. (2008). Fossil dripwater in stalagmites reveals Holocene temperature and rainfall variation in Amazonia. *Earth and Planetary Science Letters*, *275*(1–2), 54–60. https://doi.org/10.1016/j.epsl.2008.07.060

Voigt, C., Marushchak, M. E., Lamprecht, R. E., Jackowicz-Korczyński, M., Lindgren, A., Mastepanov, M., et al. (2017). Increased nitrous oxide emissions from Arctic peatlands after permafrost thaw. *Proceedings of the National Academy of Sciences*, *114*(24), 6238–6243. https://doi.org/10.1073/pnas.1702902114

Voss, M., Bange, H. W., Dippner, J. W., Middelburg, J. J., Montoya, J. P., & Ward, B. (2013). The marine nitrogen cycle: Recent discoveries, uncertainties and the potential relevance of climate change. *Philosophical Transactions of the Royal Society, B: Biological Sciences*, *368*, 20130121. https://doi.org/10.1098/rstb.2013.0121

Wang, J. K., Johnson, K. R., Borsato, A., Amaya, D. J., Griffiths, M. L., Henderson, G. M., et al. (2019). Hydroclimatic variability in Southeast Asia over the past two millennia. *Earth and Planetary Science Letters*, *525*, 115737. https://doi.org/10.1016/j.epsl.2019.115737

Wang, Y., Cheng, H., Edwards, R. L., He, Y., Kong, X., An, Z., et al. (2005). The Holocene Asian monsoon: Links to solar changes and North Atlantic climate. *Science*, *308*(5723), 854–857. https://doi.org/10.1126/science.1106296

Werner, C., Butterbach-Bahl, K., Haas, E., Hickler, T., & Kiese, R. (2007). A global inventory of N_2O emissions from tropical rainforest soils using a detailed biogeochemical model. *Global Biogeochemical Cycles*, *21*, GB3010. https://doi.org/10.1029/2006GB002909

Wolff, C., Haug, G. H., Timmermann, A., Sinninghe Damsté, J. S., Brauer, A., Sigman, D. M., et al. (2011). Reduced interannual rainfall variability in East Africa during the last ice age. *Science*, *333*(6043), 743–747. https://doi.org/10.1126/science.1203724

Wortham, B. E., Wong, C. I., Silva, L. C. R., McGee, D., Montañez, I. P., Troy Rasbury, E., et al. (2017). Assessing response of local moisture conditions in central Brazil to variability in regional monsoon intensity using speleothem 87Sr/86Sr values. *Earth and Planetary Science Letters*, *463*, 310–322. https://doi.org/10.1016/j.epsl.2017.01.034

Wurtzel, J. B., Abram, N. J., Lewis, S. C., Bajo, P., Hellstrom, J. C., Troitzsch, U., & Heslop, D. (2018). Tropical Indo-Pacific hydroclimate response to North Atlantic forcing during the last deglaciation as recorded by a speleothem from Sumatra, Indonesia. *Earth and Planetary Science Letters*, *492*, 264–278. https://doi.org/10.1016/j.epsl.2018.04.001

Xu, R., Prentice, I. C., Spahni, R., & Niu, H. S. (2012). Modelling terrestrial nitrous oxide emissions and implications for climate feedback. *New Phytologist*, *196*(2), 472–488. https://doi.org/10.1111/j.1469-8137.2012.04269.x

Xu, R., Tian, H., Lu, C., Pan, S., Chen, J., Yang, J., & Zhang, B. (2017). Preindustrial nitrous oxide emissions from the land biosphere estimated by using a global biogeochemistry model. *Climate of the Past*, *13*(7), 977–990. https://doi.org/10.5194/cp-13-977-2017-supplement

Yang, J. W., Han, Y., Orsi, A. J., Kim, S. J., Han, H., Ryu, Y., et al. (2018). Surface temperature in twentieth century at the Styx Glacier, northern Victoria Land, Antarctica, from borehole thermometry. *Geophysical Research Letters*, *45*, 9834–9842. https://doi.org/10.1029/2018GL078770

Yang, S., Chang, B. X., Warner, M. J., Weber, T. S., Bourbonnais, A. M., & Santoro, A. E. (2020). Global reconstruction reduces the uncertainty of oceanic nitrous oxide emissions and reveals a vigorous seasonal cycle. *Proceedings of the National Academy of Sciences*, *117*(22), 11,954–11,960. https://doi.org/10.1073/pnas.1921914117

Zaehle, S., Ciais, P., Friend, A. D., & Prieur, V. (2011). Carbon benefits of anthropogenic reactive nitrogen offset by nitrous oxide emissions. *Nature Geoscience*, *4*(9), 601–605. https://doi.org/10.1038/ngeo1207

Zhang, P., Cheng, H., Edwards, R. L., Chen, F., Wang, Y., Yang, X., et al. (2008). A test of climate, sun, and culture relationships from an 1810-year Chinese cave record. *Science*, *322*(5903), 940–942. https://doi.org/10.1126/science.1163965